Supporting Information

Phonon-enhanced hot carrier generation in plasmonic semiconductor systems

Yocefu Hattori[1], Jie Meng[2], Kaibo Zheng[2,3], Ageo Meier de Andrade[4], Jolla Kullgren[4], Peter Broqvist[4], Peter Nordlander[5], Jacinto Sá[1,6]*

[1] Physical Chemistry Division, Department of Chemistry, Ångström Laboratory, Uppsala University, 75120 Uppsala, Sweden

[2] Department of Chemistry, Technical University of Denmark, DK-2800 Kongens Lyngby, Denmark

[3] Chemical Physics and NanoLund, Lund University, Box 124, 22100 Lund, Sweden

[4] Structural Chemistry Division, Department of Chemistry, Ångström Laboratory, Uppsala University, 75120 Uppsala, Sweden

[5] Department of Materials Science and Engineering, Lehigh University, 5 East Packer Avenue, Bethlehem, Pennsylvania 18015, United States of America

[6] Institute of Physical Chemistry, Polish Academy of Sciences, 01-224 Warsaw, Poland
*jacinto.sa@kemi.uu.se

1. Sample Fabrication

30 NR-D Titania paste was purchased from Greatcell Solar and screen printed using a 43T mesh screen over an ultra-thin glass (ca. 0.1 mm) followed by sintering at 475^{o}C with a ramp rate of 30 ^{o}C per minute, leading to ca. 20 nm porous size mesoporous film. The sample was then immersed in a solution containing 600 □L of 0.1M HCl mixed with as prepared three ml of the Au NPs solution. Samples with different concentrations were prepared by varying the immersion time of the films in the solution. The electrostatic attraction between negatively charged particles and the positively charged TiO_2 surface drives NPs adsorption. The films were then rinsed with deionized water. Another heating step at 450 ^{o}C for 5 minutes was performed to remove the organic ligands, leading to a direct attachment of Au NPs into TiO_2. In order to diminish contact with air, a solution of PMMA diluted in acetone was spin-coated on top of the sample followed by heating at 150 ^{o}C for 15 minutes. The AuNP / ZrO_2 samples were prepared with the same procedure but by using ZrO_2 paste purchased from Solaronix instead.

The sample was fixed into a copper plate with a small aperture of 2x4 mm^2, which was heated with a temperature-controlled heater. The temperature was measured using a digital thermometer with its probe attached to the sample.

2. Transient IR Absorption Spectroscopy (TIRAS) and Transient Absorption Spectroscopy (TAS)

Briefly, 40 fs pulsed laser with 3 khz repetition rate was generated through the Libra Ultrafast Amplifier System designed by Coherent. Two optical parametric oscillators (TOPAS-prime, Light Conversion) are used to generate either the excitation beam and/or the probe light in the Mid-IR (3000-10000 nm). For measurements in the UV-NIR detector, both pump and probe lights are redirected to the Newport MS260i spectrograph with interchangeable gratings. The fundamental laser (probe, 795 nm) passes through the delay stage (1-2 fs step size) and is focused in a Sapphire optical window in order to generate visible light from 450 to 700 nm. For measurements in the Mid-IR detector, Horiba iHR 320 spectrometer is used.

The pump laser power (575 and 580 nm) was constantly monitored with less than 2% standard deviation. The timing resolution, i.e., the instrument response function is ca. 95 fs (see figure S1).

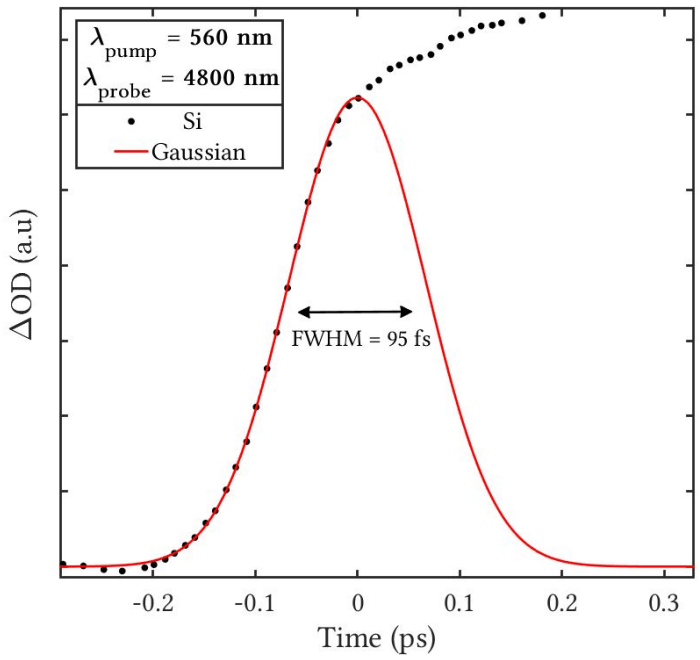

Figure S1: Transient signal from a silicon film where the rise component signal corresponded to a gaussian function with FWHM of 95 fs.

The kinetic traces were fitted with a sum of convoluted exponentials:

$$S(t) = exp[-\frac{(t-t_0)^2}{t_p}] * \sum_i A_i exp(-\frac{t-t_0}{\tau_i})$$

Where $t_p = \frac{IRF}{2ln2}$ and IRF is the width of the instrument response function (full width half maximum), t_0 is the time zero, A_i and τ_i are amplitude and decay times respectively; * is the convolution operator.

3. Power Dependence Measurements (TIRAS):

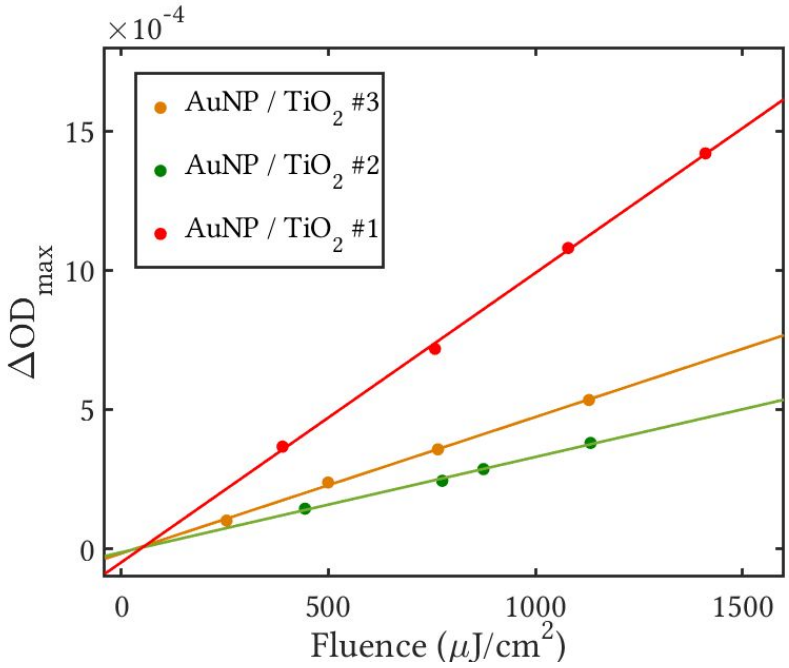

Fig. S2: Maximum ΔOD in function of excitation fluence at 580 nm of Au NPs on TiO_2 with different loading concentrations probed at 4800 nm.

4. Steady-state Absorbance measurements:

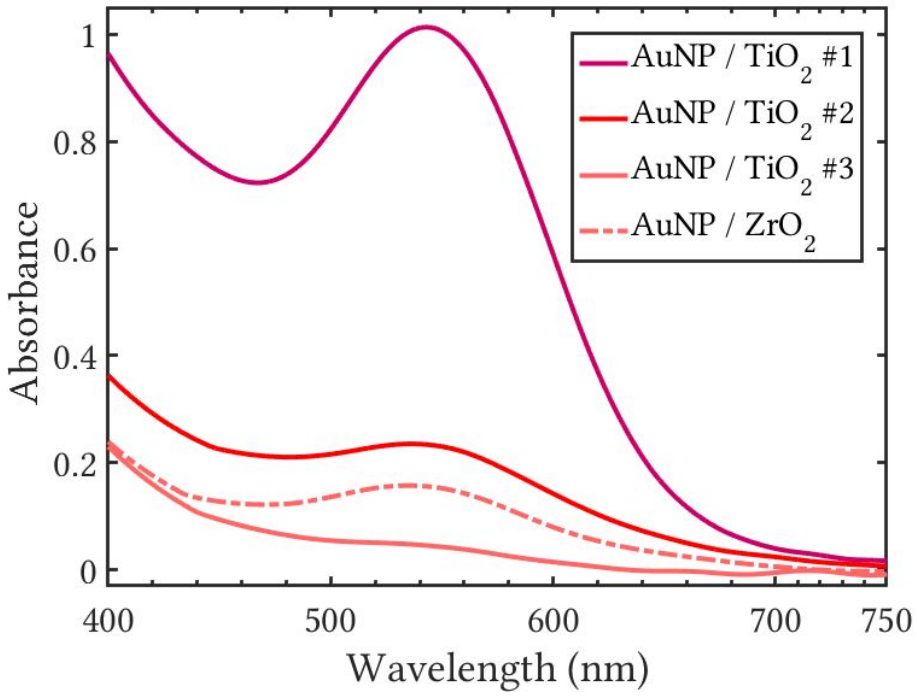

Fig.S3: Absorbance spectra of AuNP/ZrO_2 and AuNP/TiO_2 with three different concentrations.

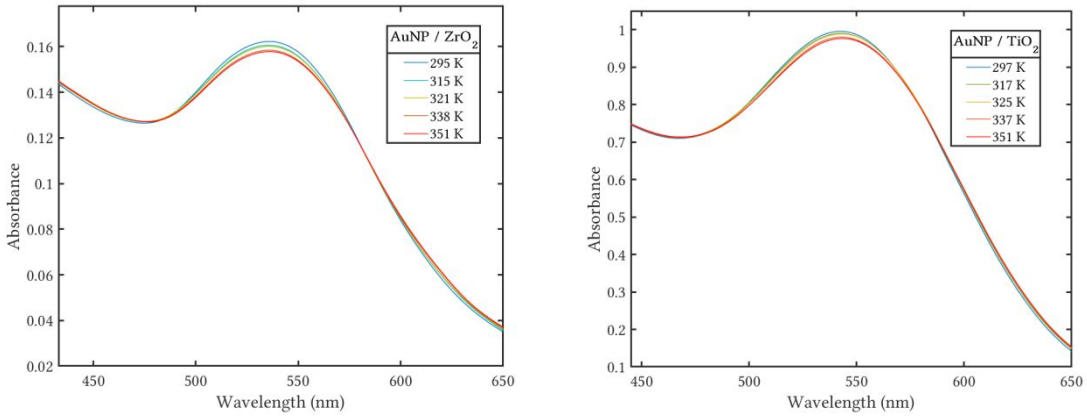

Fig. S4: Absorbance spectra of AuNP/ZrO_2 (left) and AuNP/TiO_2 (right) at different temperatures.

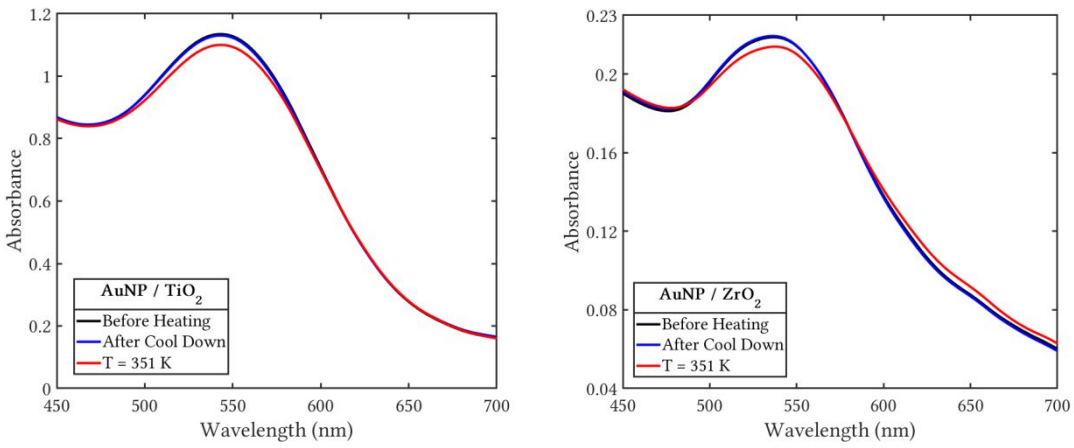

Fig. S5: Absorbance spectra of AuNP/TiO_2 and AuNP/ZrO_2 before and after exposure to different temperatures.

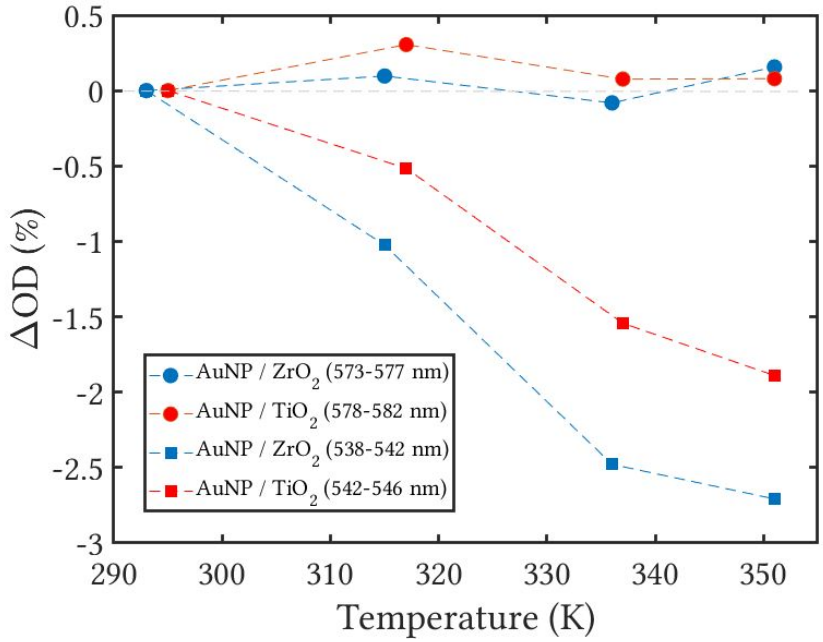

Fig. S6: Percentage of absorbance difference at the excitation wavelength and absorbance peak of AuNP/ZrO_2 and AuNP/TiO_2 in function of temperature.

5. Transmission Electron Microscopy (TEM):

The mean size distribution of Au NPs was estimated by measuring the diameter of 313 particles of the TEM pictures depicted below.

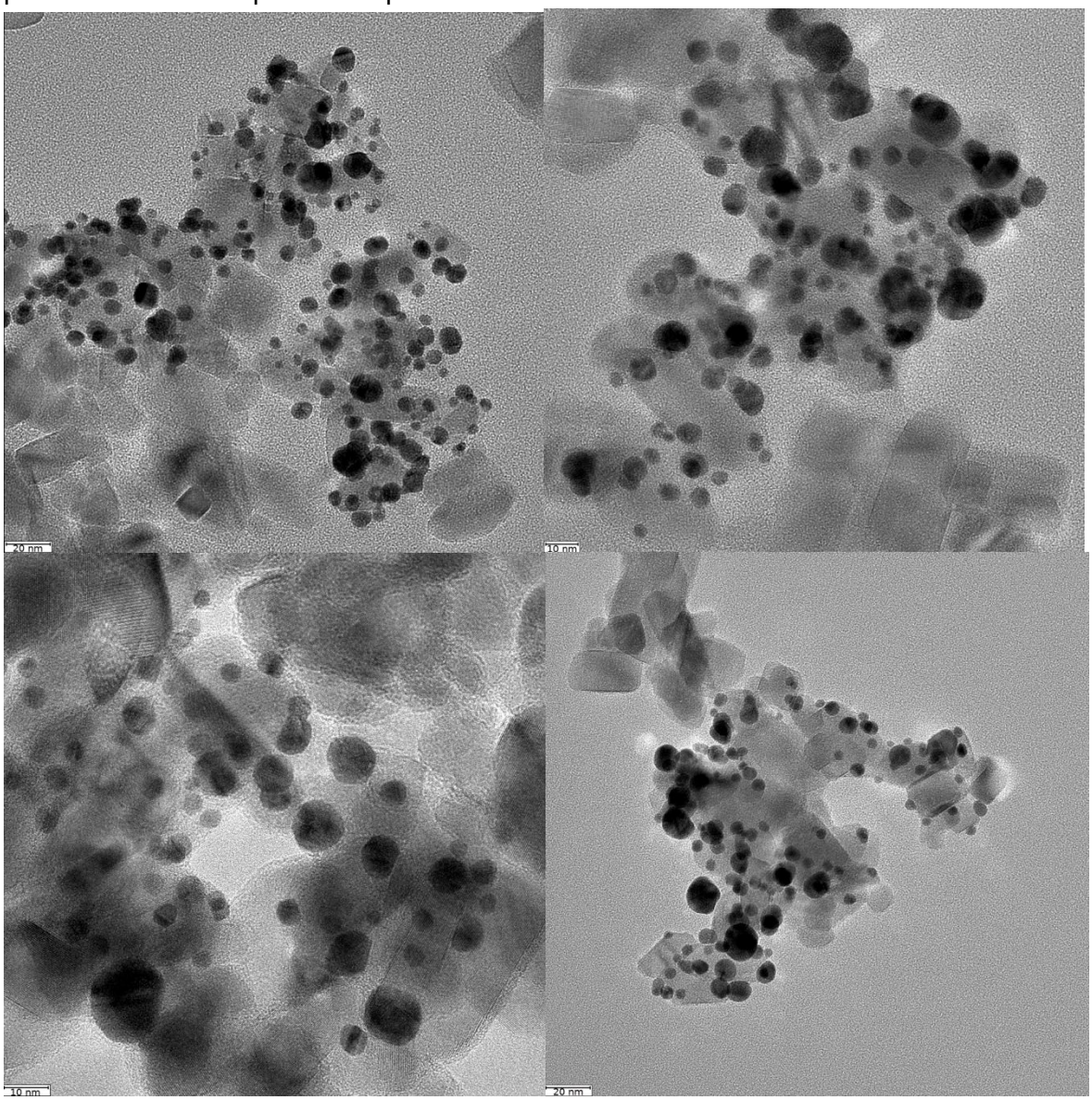

Fig. S7: TEM pictures obtained from the sample AuNP/TiO_2.

6. e-e and e-ph scattering rates

The Drude damping factor Γ depends on both e-e and e-ph mechanisms. The expression for the temperature dependence of the collision process between electrons is obtained by employing Born approximation and the Thomas-Fermi screening of Coulomb interaction [1,2]

$$\Gamma_{e-e}(T,\lambda) = \frac{\pi^3 \Delta \Gamma}{12 h E_F}\left[(k_B T)^2 + \left(\frac{hc}{\lambda}\right)^2\right]$$

Where $\Gamma = 0.55, \Delta = 0.77$ and $E_F = 5.5\ eV$ are the average scattering probability over the Fermi surface, the fractional Umklapp scattering and the fermi energy of free electrons.
Holstein [3,4] derived the expression for e-ph scattering by assuming free electrons without Umklapp collisions and single Debye model phonon spectrum:

$$\Gamma_{e-ph}(T) = \Gamma_0\ \left[\frac{2}{5} + 4\left(\frac{T}{\theta_D}\right)^5 \int_0^{\frac{\theta_D}{T}} \frac{z^4}{e^z - 1} dz\ \right]$$

For Au, the Debye's temperature is $\theta_D = 170\ K$ and Γ_0= 0.07 eV which is determined by fitting the bulk permittivity at frequencies below the interband transition.

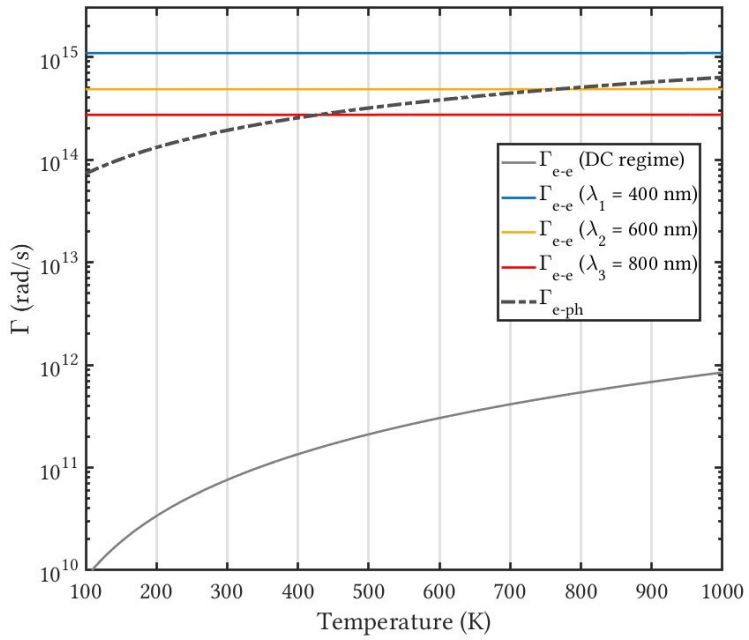

Fig. S8: Temperature dependence of the scattering rate for e-e and e-ph scattering.

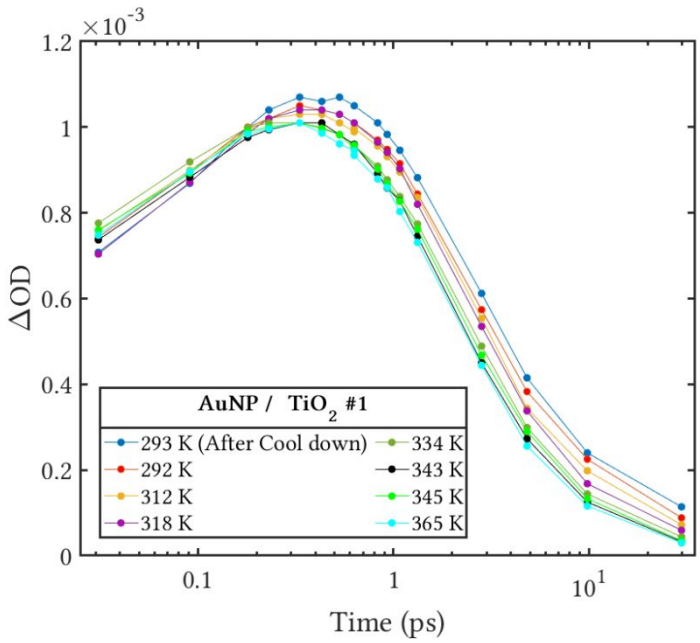

Fig. S9: Kinetic traces of the data presented in figure 4a.

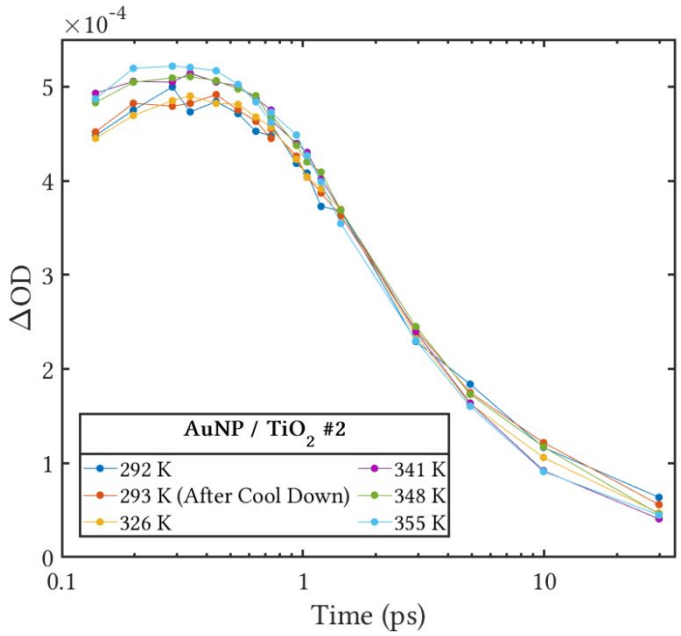

Fig. S10: Kinetic traces of the data presented in figure 4b.

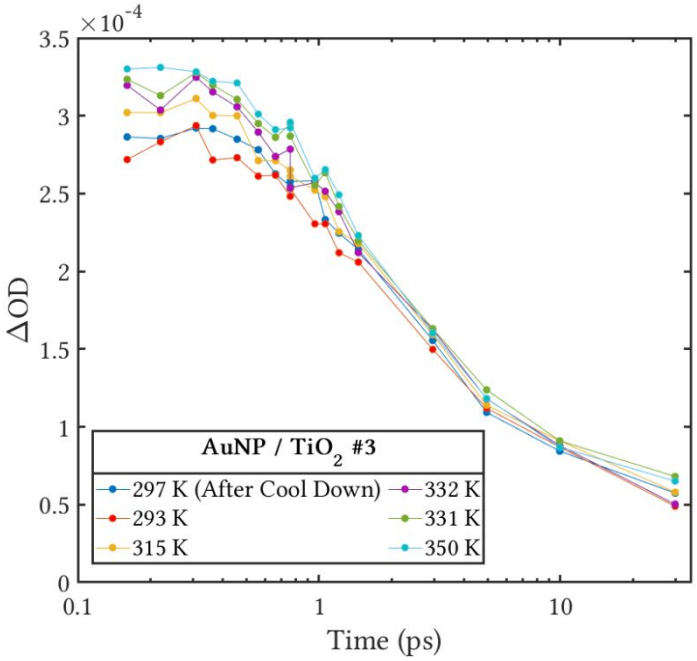

Fig. S11: Kinetic traces of the data presented in figure 4c.

7. Tauc plot in function of temperature of TiO_2 films

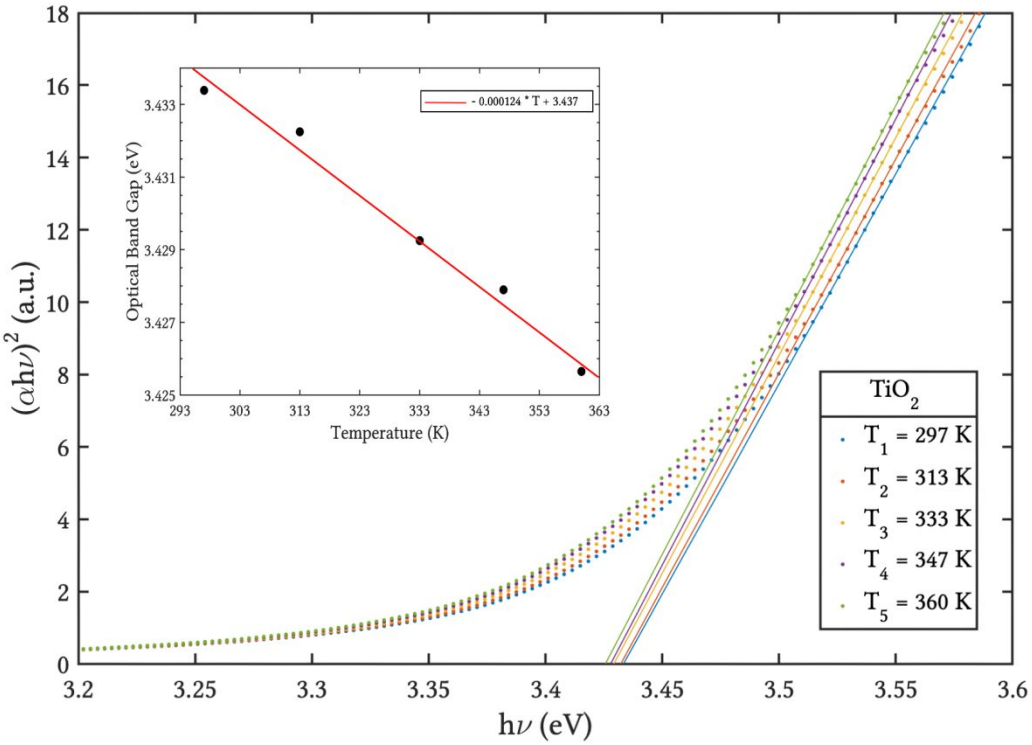

Fig S12: Tauc plot of TiO_2 at different temperatures. Inset: Obtained optical band-gap in function of temperature.

8. Theoretical simulations on the effect of phonons on Schottky barrier

To simulate the effect that phonons have on the interface dipole at the Au/TiO_2 interface, we have performed ab initio molecular dynamics simulations for an Au/TiO2 model. The model was constructed from the experimental lattice constant of anatase TiO_2. A supercell was generated by cleaving the (101) surface, which is deemed to be the most stable surface for anatase TiO_2. To minimize the strain in the Au part, we found that the best match was to use an anatase 2x2 (101) in conjunction with a rotated Au (110) surface, as illustrated in Fig. S12a. the model consists of 144 atoms in total.

The simulations were made using the density functional theory in the implementation with plane-waves and pseudopotentials using the Vienna Ab Initio Simulation Package (VASP) [5-8]. The calculations were performed using the PBE density functional [9,10] in conjunction with the rotationally invariant Hubbard correction of Dudarev et al. [11]. We used a U-value of 5 eV for Ti(d) states. To treat the electron-core interactions. we used projected augmented wave (PAW) pseudopotentials [12,13], explicitly accounting for 11 Au (s1d10), 4 Ti (d3s1), and 6 O (s2p4) valence electrons. The plane-wave basis set was truncated by a kinetic energy cut-off of 600 eV, and the Brillouin zone was sampled at the Gamma point. The Molecular dynamics simulations were performed using the Verlet algorithm in the NVE ensemble. The time step was set to 1fs. After an equilibration time of approximately 2ps, the temperature was found to be stable enough for data collecting. The average local potential across the interface, see Fig. S12b, were sampled every 100 fs.

The Schottky barrier (SB) can be calculated through the following equation:

$$SB = V_{avg}^{ox,\,interface} + (V_{avg}^{ox,\,bulk} - CB^{ox,\,bulk}) - V_{avg}^{Au,\,interface} + (V_{avg}^{Au,\,bulk} - E^{fermi,\,bulk}) \quad \text{(S1)}$$

Where $V_{avg}^{ox,\,interface}$ and $V_{avg}^{Au,\,interface}$ are the average potentials in the center of the TiO_2 and the Au parts of the interface model (c.f. Fig .S12a and S12b), and $(V_{avg}^{ox,\,bulk} - CB^{ox,\,bulk})$ and $(V_{avg}^{Au,\,bulk} - E^{fermi,\,bulk})$ are the position of the conduction band (CB) and the Fermi level $E^{fermi,\,bulk}$ of bulk anatase TiO_2 and bulk Au, respectively. As these contributions are constant, the fluctuation in the Schottky barrier can be sampled by computing the ΔV_{avg} between the TiO_2 and the Au components directly, i.e. by mapping fluctuations in the interface dipole.

The $\Delta V_{avg}$with respect to the T= 0 K model for a series of temperatures is shown in Fig. S13. The results show that in the interesting temperature regime, T=300-350K, the Schottky barrier is expected to increase approximately 0.11 eV. This is similar to the experimental values reported by Mahoto and Puigdollers for other Au/TM interfaces [14].

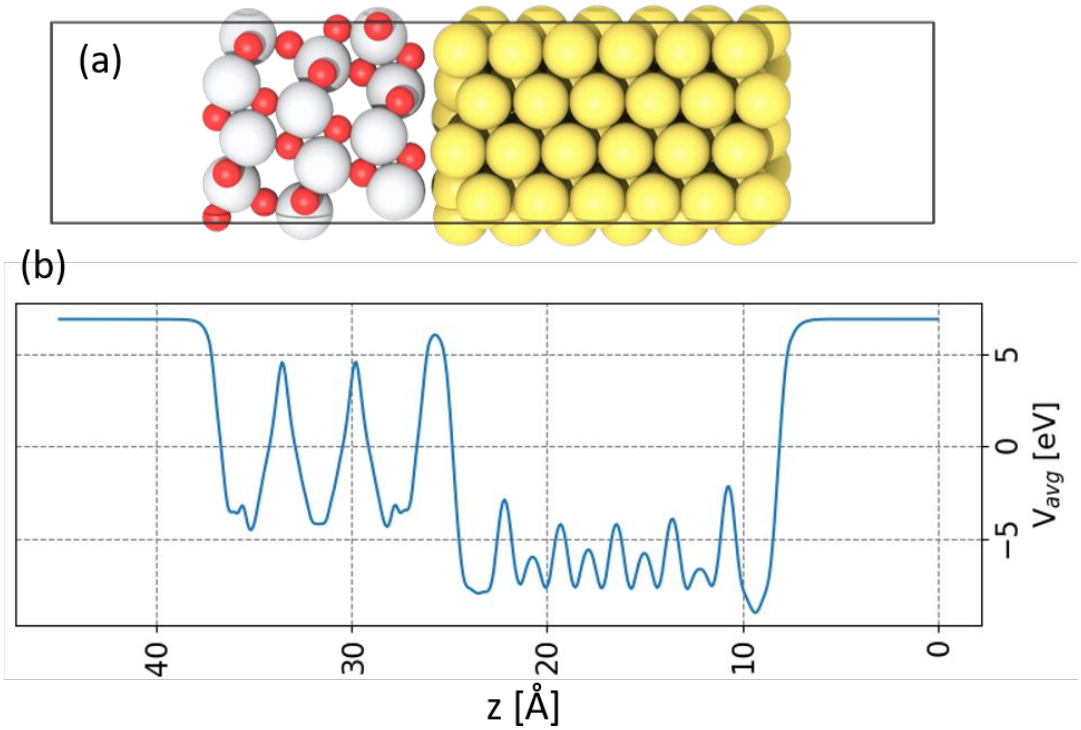

Fig S13: (a) atomistic model of the Au/TiO2 interface. The lateral lattice constants are chosen according to the experimental anatase TiO_2 101 surface. The best match for Au was found to be a rotated (110) surface. The strain in the Au part is however not deemed to affect the results concerning temperature-dependent shifts in the computed SB in a significant manner. (b) averaged electrostatic potential across the Au/TiO_2 interface at T=0K.

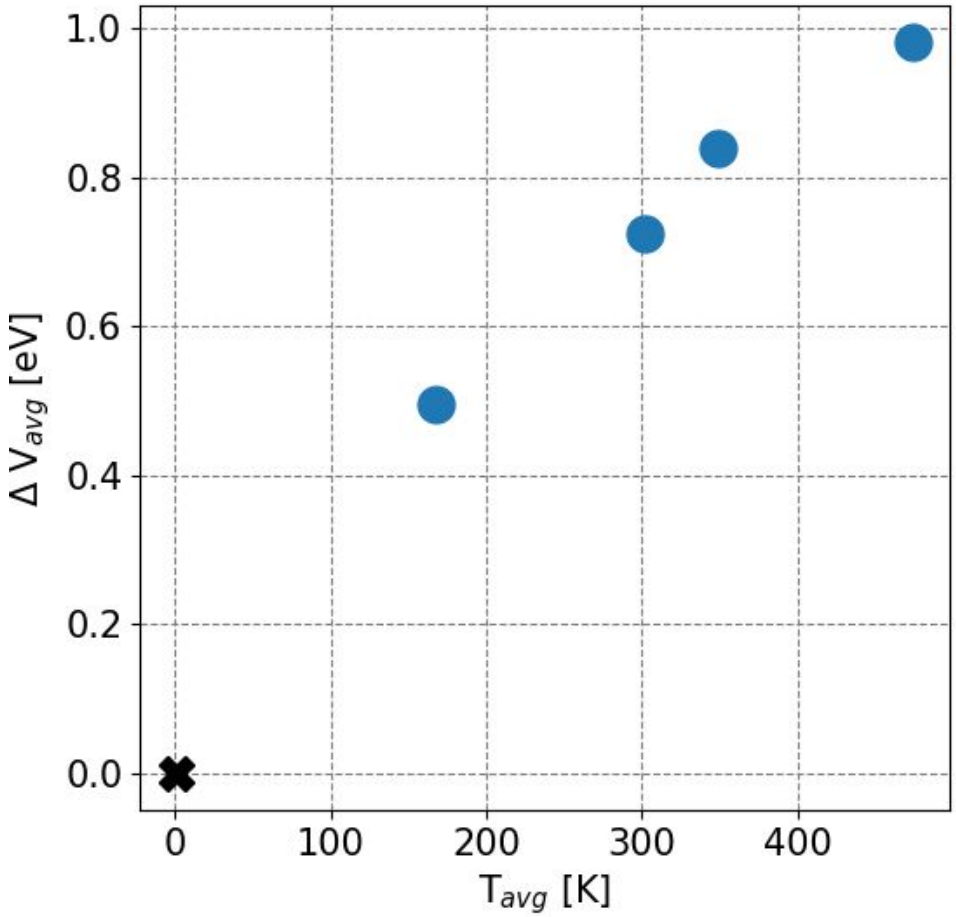

Fig S14: Shift in Schottky barrier due to thermal effects at the TiO2/Au interface from molecular dynamics simulations. The shift is obtained by studying the effect temperature has on the interface dipole and is calculated according to Eq. S1 and by subtracting the ΔV_{avg} obtained for 0K (indicated by the black cross). The blue points are obtained by averaging the ΔV_{avg} a time period of 2 ps.

9. References:

[1] W.E. Lawrence, Phys. Rev. B **13**, 5316 (1976).
[2] W.E. Lawrence, J.W. Wilkins, Phys. Rev. B **7**, 2317 (1973).
[3] T. Holstein, Phys. Rev. **96**, 535 (1954).
[4] T. Holstein, Ann. Phys. **29**, 410 (1964).
[5] G. Kresse and J. Hafner, Phys. Rev. B **47**, 558 (1993).
[6] G. Kresse and J. Furthmüller, Phys. Rev. B **54**, 11169 (1996).
[7] G. Kresse and J. Furthmüller, Comput. Mater. Sci. **6**, 15 (1996).
[8] G. Kresse and J. Hafner, Phys. Rev. B **49**, 14251 (1994).
[9] J. P. Perdew, K. Burke, and M. Ernzerhof, Phys. Rev. Lett. **77**, 3865 (1996).
[10] J. P. Perdew, K. Burke, and M. Ernzerhof, Phys. Rev. Lett. **78**, 1396 (1997).
[11] S. L. Dudarev, G. A. Botton, S. Y. Savrasov, C. J. Humphreys, and A. P. Sutton, Phys. Rev. B **57**, 1505 (1998).
[12] P. E. Blöchl, Phys. Rev. B **50**, 17953 (1994).
[13] G. Kresse and D. Joubert, Phys. Rev. B **59**, 1758 (1999).
[14] S. Mahato and J. Puigdollers, Phys. B Condens. Matter **530**, 327 (2018).